

## Supporting Information

### **Intrinsic magnetic characteristics dependent charge transfer and properties for photocatalytic HER over Fe<sub>3</sub>O<sub>4</sub>@PPy@Pt catalyst under visible light irradiation**

State Key Laboratory for Oxo Synthesis and Selective Oxidation, Lanzhou Institute of Chemical Physics, Chinese Academy of Sciences, Lanzhou, 730000, China.  
College of Material Engineering, Jinling Institute of technology, Nanjing, China

\*Corresponding author: E-mail: [gxlu@lzb.ac.cn](mailto:gxlu@lzb.ac.cn)

#### **1 Experimental detail**

##### **1.1 Preparation of Fe<sub>3</sub>O<sub>4</sub> micro-spheres**

The mono-dispersed Fe<sub>3</sub>O<sub>4</sub> micro-spheres were synthesized by a one-pot hydrothermal method. In a typical synthesis, FeCl<sub>3</sub>·6H<sub>2</sub>O (0.54 g), sodium citrate (1.2 g), and urea (0.2 g) were dissolved in distilled water (40 mL). Then, PAAS (0.2 g) was added under continuous stirring until it was totally dissolved. The solution was transferred to a 50 mL Teflon-lined autoclave, which was then sealed and maintained at 200°C for 12 h. The product was separated by magnetic separation, washed with distilled water and absolute ethanol several times, and then dried in a vacuum oven at 60 °C overnight.

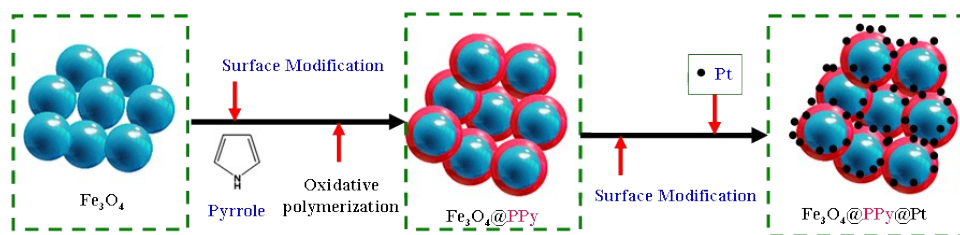
##### **1.2 Preparation of Fe<sub>3</sub>O<sub>4</sub>@Pt catalysts**

The Fe<sub>3</sub>O<sub>4</sub>@Pt catalysts were synthesized by microwave method. In a typical synthesis, 0.2 g prepared Fe<sub>3</sub>O<sub>4</sub> micro-spheres and 0.2 g poly(N-vinylpyrrolidone) (PVP) (K<sub>30</sub>) were re-dispersed into 40 mL distilled water via ultrasound. Then 20 mL ethylene glycol was dissolved into the above-prepared solution under vigorous stirring. Then 1 mL aqueous K<sub>2</sub>PtCl<sub>6</sub> (Pt: 2 mg/mL) was added into above solution subsequently. The solution was transferred to a 50 mL round-bottomed flask, which was then sealed and reacted under 800 W microwaves for 5 min with condensing reflux. The product was separated by magnetic separation, washed with distilled water and absolute ethanol several times, and then dried in a vacuum oven at 60 °C overnight.

##### **1.3 Preparation of Fe<sub>3</sub>O<sub>4</sub>@PPy**

The Fe<sub>3</sub>O<sub>4</sub>@PPy were synthesized by oxidative polymerization of pyrrole (Py), as shown in scheme S1. In a typical synthesis, 0.2 g prepared Fe<sub>3</sub>O<sub>4</sub> micro-spheres and 0.05 g polyvinylpyrrolidone (PVP) (K<sub>30</sub>) were re-dispersed into 40 mL distilled water via ultrasound. 0.108 g FeCl<sub>3</sub> and 50 mL Py were sequentially added to the solution under vigorous ultrasound vibration. After reacting for 2 h, the product was separated by magnetic separation, washed with distilled water and absolute ethanol several times, and then dried in a vacuum oven at 60°C overnight.

##### **1.4 Preparation of Fe<sub>3</sub>O<sub>4</sub>@PPy@Pt catalysts**



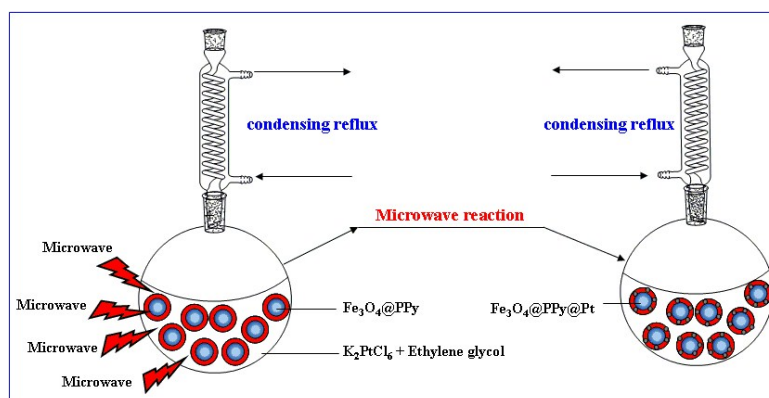
**Scheme S1 Two-step routine route for the synthesis of photo-catalysts**

The  $\text{Fe}_3\text{O}_4@\text{PPy}@Pt$  catalysts are all prepared by two-step routine, as shown Scheme S1. Firstly, the  $\text{Fe}_3\text{O}_4@\text{PPy}$  spheres were synthesized by oxidative polymerization of pyrrole (Py). The PPy shell wrapped the  $\text{Fe}_3\text{O}_4$  spheres to form a core-shell structure. Secondly, Pt dots are introduced into the PPy layer by microwave method to form the  $\text{PPy}@Pt$  shell with various Pt dots.

#### 1.4.1 Preparation of $\text{Fe}_3\text{O}_4@\text{PPy}@Pt$ catalysts

The  $\text{Fe}_3\text{O}_4@\text{PPy}@Pt$ -A was synthesized by microwave method, as shown in scheme S2. 0.2 g prepared  $\text{Fe}_3\text{O}_4@\text{PPy}$  and 0.05 g PVP ( $\text{K}_{30}$ ) were re-dispersed into 20 mL distilled water via ultrasound. Then 20 mL ethylene glycol was dissolved into the above-prepared solution under vigorous stirring. Then 1 mL aqueous  $\text{K}_2\text{PtCl}_6$  (Pt: 2 mg/mL) was added into above solution subsequently. The solution was transferred to a 50 mL round-bottomed flask, which was then sealed and reacted under 800 W microwaves for 5 min with condensing reflux. The product was separated by magnetic separation, washed with distilled water and absolute ethanol several times, and then dried in a vacuum oven at 60 °C overnight.

Microwave heating is based on the interaction of matter with electromagnetic radiation.<sup>S1</sup> It is independent of the thermal conductivity of the surrounding materials and allows an instantaneous on/off switching of the heating. During the reactive process, microwave radiation just affects the rotation of dipoles and induces translational motion of free or bound charges within the reaction media. In consequence, the method exhibits special advantages, including rapid synthesis kinetics, improving the uniformity, dispersion and phase purity of nano-materials<sup>S1, S2</sup>.



**Scheme S2 Synthesis of  $\text{Fe}_3\text{O}_4@\text{PPy}@Pt$  catalysts by microwave method**

## Characterization Details

Transmission electron microscopy (TEM) and high-resolution TEM (HRTEM) were taken with a Tecnai-G2-F30 field emission transmission electron microscope operating at an accelerating voltage of 300 kV. X-ray diffraction (XRD) patterns of the samples were recorded on a Rigaku B/Max-RB diffractometer with a nickel filtrated Cu K $\alpha$  radiation operated at 40 kV and 40mA. X-ray photoelectron spectroscopy (XPS) analysis was performed using a VG Scientific ESCALAB210-XPS photoelectron spectrometer with an Mg K $\alpha$  X-ray resource. Raman spectra were performed in air by high-resolution confocal  $\mu$ -Raman system (Horiba JY, LabRam HR800).

FT-IR spectra were measured on a Nexus 870 FT-IR spectrometer from KBr pellets as the sample matrix. The fluorescence decay time were measured using the Horiba Jobin Yvon Data Station HUB operating in time-correlated single photon counting mode (TCSPC) with the time resolution of 200 ps. Nano LED diode emitting pulses at 460 nm with 1 MHz repetition rate was used as an excitation source. The amount of hydrogen evolution was measured using gas chromatograph (Agilent 6820, TCD, 13 $\times$ column, Ar carrier). Photon flux of the incident light was determined using a Ray virtual radiation actinometer (FU 100, silicon ray detector, light spectrum, 400-700 nm; sensitivity, 10-50  $\mu\text{mol}^{-1}\cdot\text{m}^{-2}\cdot\text{s}^{-1}$ ).

## 3 Results details

### 3.1 Recycle HER experiment over the Fe<sub>3</sub>O<sub>4</sub>@PPy@Pt-C catalyst

Fig. S1 shows four recycles of HER over the Fe<sub>3</sub>O<sub>4</sub>@PPy@Pt-C catalyst. The H<sub>2</sub> evolution remains 75.15% after four times recycling. Fig. S2 is the Pt 4f XPS spectra before and after four recycle of HER reaction. The XPS Pt 4f spectra shows that the tiny Pt NPs are still in metal state after four times recycling, indicating that the Pt NPs are stable during the HER reaction.

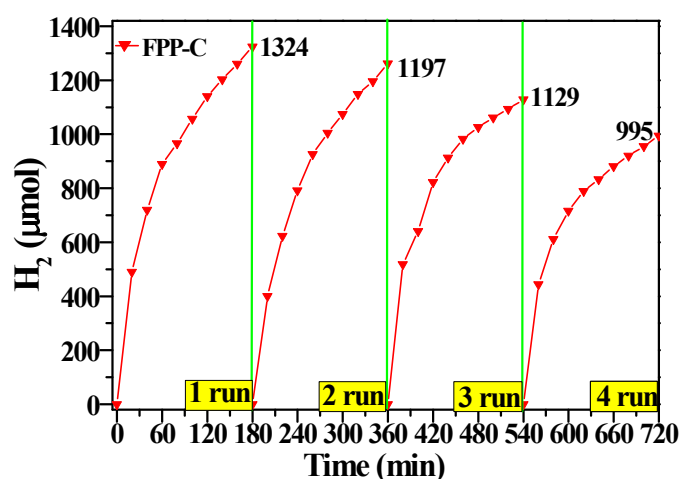


Fig. S1 Four recycles of HER over the Fe<sub>3</sub>O<sub>4</sub>@PPy@Pt-C catalyst

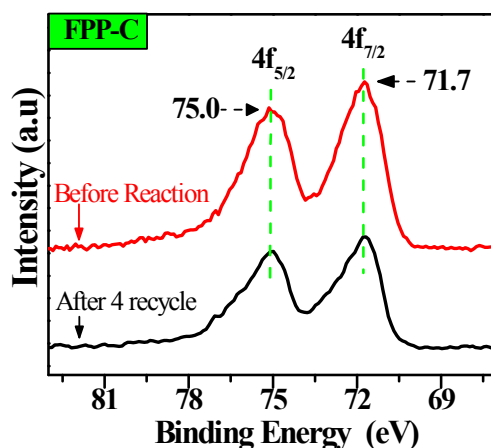


Fig. S2 Pt 4f spectra of  $\text{Fe}_3\text{O}_4@\text{PPy}@\text{Pt-C}$   
 (a) before and (b) after four recycle of HER reaction

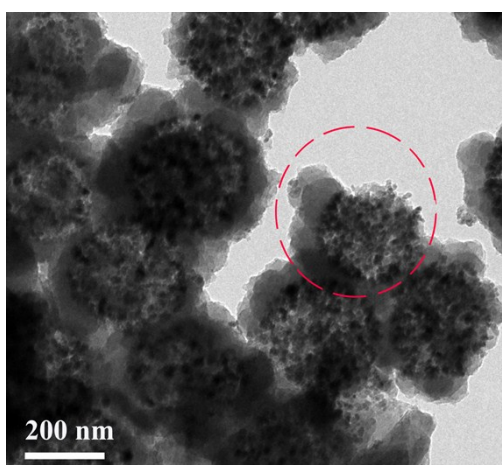


Fig. S3 TEM image of  $\text{Fe}_3\text{O}_4@\text{PPy}@\text{Pt-C}$  after four recycle of HER reaction

The degradation of catalytic activity after 140 min reaction could be assigned to two reasons: the consumption of sacrificial donor and the breaking of  $\text{Fe}_3\text{O}_4@\text{PPy}@\text{Pt}$  catalysts. On one hand, tri-ethanolamine (TEOA) plays the role as sacrificial donor and the consumption of TEOA could slow down the electron transfer between the EY and catalyst, as a result declining the photo-catalytic  $\text{H}_2$  evolution activity of catalysts [S6, S7]. On the other hand, some  $\text{Fe}_3\text{O}_4@\text{PPy}@\text{Pt-C}$  catalysts were partially broken after four times recycling (Fig. S3), thus the photo-generated electrons could not be transferred effectively from the EY dye to the Pt dots inside the PPy shell.

### 3.7 BET analysis

BET tests have been supplemented to investigate the specific surface area of the three modified catalysts. The nitrogen adsorption-desorption isotherms of all samples exhibited the IV type with H3 type hysteresis loop (Fig. S4). Specific surface area of the  $\text{Fe}_3\text{O}_4@\text{PPy}@\text{Pt-A}$ ,  $\text{Fe}_3\text{O}_4@\text{PPy}@\text{Pt-B}$  and  $\text{Fe}_3\text{O}_4@\text{PPy}@\text{Pt-C}$  catalysts are 21.8, 22.0, and 20.5  $\text{m}^2\text{g}^{-1}$ , respectively

(Tab. S1, data obtained from BET method). The approximate values indicate that the specific surface area has little effect on the photo-catalytic activity of catalysts.

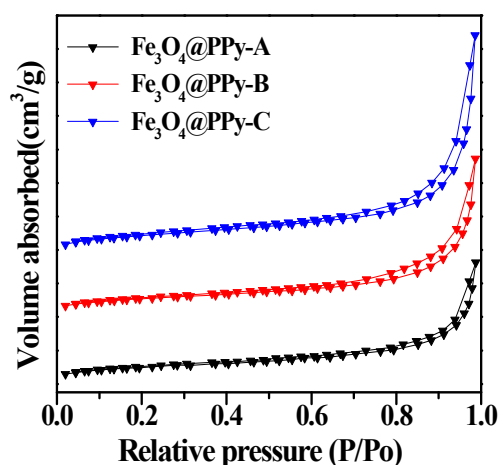


Fig. S4 Nitrogen adsorption-desorption isotherms of all samples

**Tab. S1** Structural parameters obtained from N<sub>2</sub> adsorption isotherms analysis ()

Samples	$S_{\text{BET}}$ (m <sup>2</sup> g <sup>-1</sup> ) <sup>a</sup>
Fe <sub>3</sub> O <sub>4</sub> @PPy@Pt-A	21.8
Fe <sub>3</sub> O <sub>4</sub> @PPy@Pt-B	22.0
Fe <sub>3</sub> O <sub>4</sub> @PPy@Pt-C	20.58

<sup>a</sup> Obtained from BET method

### 3.6 Lifetime of the photo-catalysts

Table S2 Decay parameters of EY in the presence of Fe<sub>3</sub>O<sub>4</sub>@Pt and Fe<sub>3</sub>O<sub>4</sub>@PPy@Pt

System	Lifetime (ns)	Pre-exponential factors		
		A	A	$\chi^2$
EY	$\tau=1.23$	0.0727	0.428	1.00
Fe <sub>3</sub> O <sub>4</sub> @PPy	$\tau_1=0.983, \tau_2=2.031$	A1=0.0716, A2=0.00914	0.551	1.00
Fe <sub>3</sub> O <sub>4</sub> @Pt	$\tau_1=0.927, \tau_2=1.67$	A1=0.0654, A2=0.0173	0.506	1.00
Fe <sub>3</sub> O <sub>4</sub> @PPy@Pt-2	$\tau_1=0.956, \tau_2=1.787$	A1=0.0683, A2=0.0128	0.403	1.00
Fe <sub>3</sub> O <sub>4</sub> @PPy@Pt-3	$\tau_1=0.995, \tau_2=2.027$	A1=0.0715, A2=0.00868	0.373	1.00
Fe <sub>3</sub> O <sub>4</sub> @PPy@Pt-4	$\tau_1=1.094, \tau_2=2.626$	A1=0.0714, A2=0.00492	0.456	1.00
Fe <sub>3</sub> O <sub>4</sub> @PPy@Pt-5	$\tau_1=1.003, \tau_2=2.114$	A1=0.0740, A2=0.00723	0.459	1.00

Fluorescence lifetime of EY was investigated to reveal more information about the energy transfer process (Table S2). The emission of EY exhibits a single-exponential decay and its lifetime is 1.23 ns. The single-exponential decay divided into a short and a long exponential decay when the Fe<sub>3</sub>O<sub>4</sub>@Pt or the Fe<sub>3</sub>O<sub>4</sub>@PPy@Pt catalyst was tested (Table S2). The long and short emission decay could respectively be assigned to the unbounded EY and the EY linked to the catalyst.<sup>S6</sup> It is apparent that the EY- Fe<sub>3</sub>O<sub>4</sub>@PPy@Pt exhibits longer fluorescence lifetime than the EY-Fe<sub>3</sub>O<sub>4</sub>@Pt system, indicating that the PPy layer could prolong the lifetime of excited EY

in the TEOA solution.<sup>S7</sup> Longer lifetime could leave more time for the photo-electrons to pass through the PPy shell before being quenched by the sacrifice reagent TEOA, as a result improving the H<sub>2</sub> evolution.

### 3.5 Fe 2p XPS spectra of the photo-catalysts

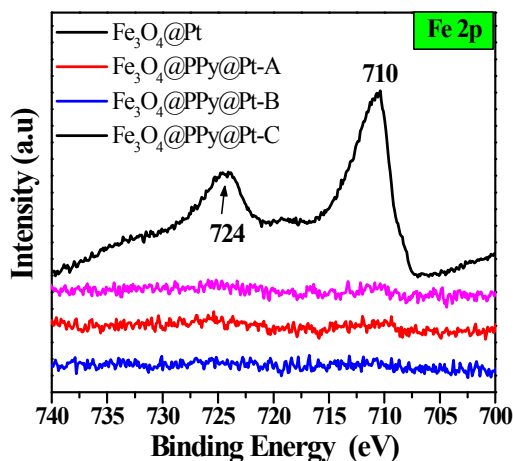


Fig. S5 Fe 2p spectra of Fe<sub>3</sub>O<sub>4</sub>@Pt, Fe<sub>3</sub>O<sub>4</sub>@PPy@Pt-A, Fe<sub>3</sub>O<sub>4</sub>@PPy@Pt-B, and Fe<sub>3</sub>O<sub>4</sub>@PPy@Pt-C

The Fe 2p XPS spectra of Fe<sub>3</sub>O<sub>4</sub>@PPy@Pt indicate that the surfaces of Fe<sub>3</sub>O<sub>4</sub> microspheres have been covered by the PPy@Pt layer (Fig. S6).

### 3.2 Detailed assignments of the Raman bands

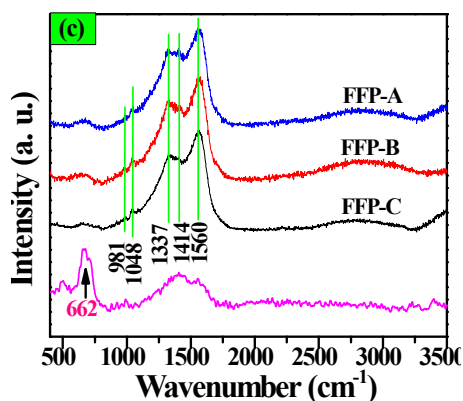


Fig. 3 (c) Raman spectra of Fe<sub>3</sub>O<sub>4</sub>@Pt and Fe<sub>3</sub>O<sub>4</sub>@PPy@Pt

Tab. S3 Assignments of the Raman bands

Wavenumber (cm <sup>-1</sup> )	Assignment
1560	stretching vibrations of C=C
1454	C-N bond in the pyrrole ring
1414	COO <sup>-</sup> symmetric
1337	C-H stretching vibration
1048	C-H in plane bending vibration
981	Ring deformation associated with bipolaron
662	Fe-O stretching vibration

### 3.3 N 1s spectra of photo-catalysts

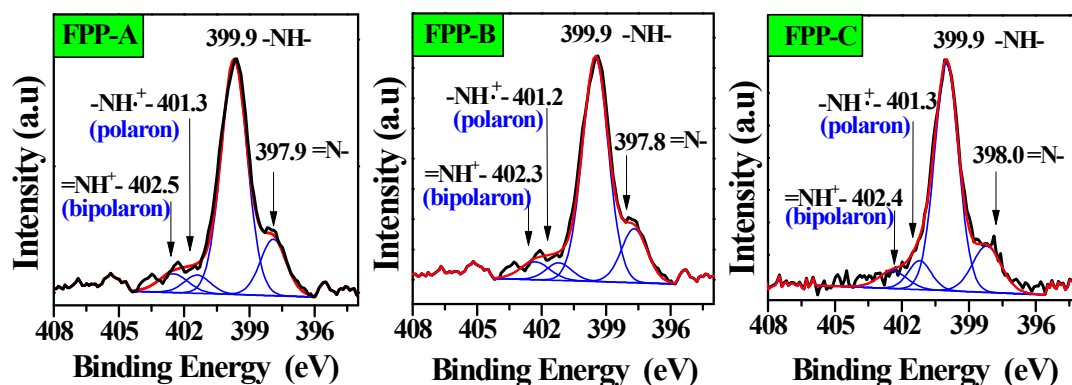
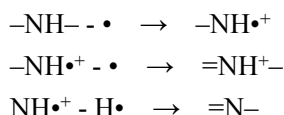


Fig. S6 N 1s spectra of Fe<sub>3</sub>O<sub>4</sub>@PPy@Pt-A, Fe<sub>3</sub>O<sub>4</sub>@PPy@Pt-B and Fe<sub>3</sub>O<sub>4</sub>@PPy@Pt-C

The N 1s spectra was investigated to reveal more information of the PPy shell, in which there exist the neutral N (-NH-), polaron (-NH<sup>•+</sup>-), bipolaron (=NH<sup>+</sup>-) and imine-like nitrogen (=N-) groups (Fig. S1). The strongest peaks at 399.8 and 399.9 eV are attributed to the -NH- groups in pyrrole ring. The existence of =N-, -NH<sup>•+</sup>- and =NH<sup>+</sup>- groups indicates that the oxidation state and de-protonation of the PPy shell<sup>S3, S4</sup>:



The -NH<sup>•+</sup>- and =NH<sup>+</sup>- groups in Fe<sub>3</sub>O<sub>4</sub>@PPy@RGO are much less than that in the Fe<sub>3</sub>O<sub>4</sub>@PPy, indicating the strong interaction between the PPy layers and the RGO sheets. Some electrons may transfer from the graphene sheets to the PPy layers by  $\pi$ - $\pi$  interactions and reduce the positively charged -NH<sup>•+</sup>-, =NH<sup>+</sup>- groups to their neutral state -NH-. The electrons transfer between the PPy and RGO could help to connect the Fe<sub>3</sub>O<sub>4</sub>@PPy more firmly with the RGO sheets by delocalized electrons.

### 3.4 C 1s spectra of photo-catalysts

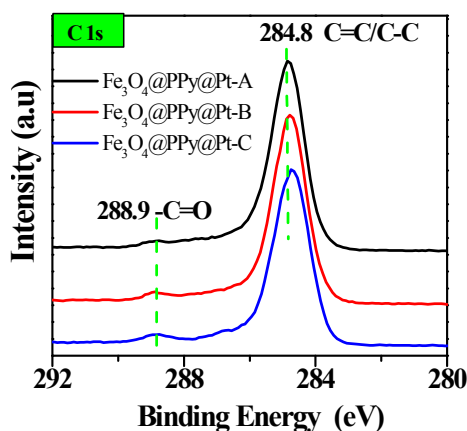


Fig. S7 C 1s spectra of Fe<sub>3</sub>O<sub>4</sub>@PPy@Pt-A, Fe<sub>3</sub>O<sub>4</sub>@PPy@Pt-B and Fe<sub>3</sub>O<sub>4</sub>@PPy@Pt-C

In Fig. S7, the peaks at 284.8 and 288.9 eV verify the existence of C=C and C=O bonds.

Intensity of the C-O and C=O groups is much lower than that of the C=C groups, indicating that the surface of PPy shell are mainly composed of C=C conjugated bonds.

### 3.4 O 1s spectra of photo-catalysts

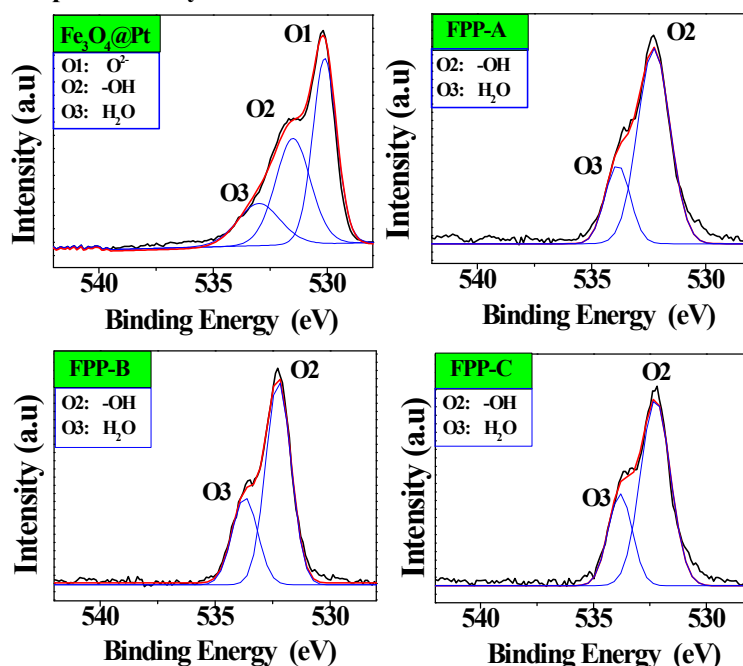


Fig. S8 O 1s spectra of  $\text{Fe}_3\text{O}_4@\text{Pt}$  and  $\text{Fe}_3\text{O}_4@\text{PPy}@\text{Pt}$

The O 1s spectra are also investigated to reveal more information of the surface state. The O 1s spectra of photo-catalysts could be de-convoluted into three peaks around 530, 531 and 533 eV, which respectively corresponds to the oxygen in the  $\text{Fe}_3\text{O}_4$  crystal lattice oxide oxygen ( $\text{O}^{2-}$ ), hydroxyl ( $-\text{OH}$ ), and absorbed water ( $\text{H}_2\text{O}$ ).<sup>S5</sup> The  $\text{O}^{2-}$  species almost disappear for the  $\text{Fe}_3\text{O}_4@\text{PPy}@\text{Pt}$  catalysts, indicating that the surface of  $\text{Fe}_3\text{O}_4$  microspheres and the defects on the surface are wholly covered by the PPy layer. The layer can protect the photo-generated electrons from being quenched by the surface defects of  $\text{Fe}_3\text{O}_4$ .

### Reference

- (S1) Schwenke, A. M.; Hoepfner, S.; Schubert U. S. *Adv. Mater.* **2015**, 27, 4113.  
(S2) Cho, H. Y.; D. A. Yang,; Kim, J.; Jeong, S. Y.; Ahn W. S. *Catalysis Today* **2012**, 185, 35.  
(S3) Yao, T. J.; Zuo, Q.; Wang, H.; et al. *J. Colloid Interface Sci.* **2015**, 450, 366.  
(S4) Ruangchuay, L.; Schwank, J; Sirivata, A.; et al. *Appl. Surf. Sci.* **2002**, 199, 128.  
(S5) Hu, X.; Ma, M.; Zeng, M.; Sun, Y.; Chen, L.; Xue, Y.; Zhang, T.; Ai, X.; Mendes, R.; Rummeli, M.; Fu, L. *Appl. Mater. Interfaces* **2014**, 6, 22527.  
(S6) Min, S.; Lu, G. *J. Phys. Chem. C.* **2011**, 115, 13938.  
(S7) Bhargava, G.; Gouzman, I.; Chun, C.; Ramanarayanan, T.; Bernasek, S.; *Appl. Surf. Sci.* **2007**, 253, 4322.  
(S8) Brillouin L., *Phys. Rev.* **1945**, 67, 260.